Supplementary Information

Title

Passivation Mechanism of Perovskite Upper Interface based on $MAPbBr_3$ Quantum Dots for Efficient and Stable Perovskite Solar Cells

Author(s), and Corresponding Author(s)*

Yan Feng, [a] *Huilin Li,* [a] *Zhitao Shen,* [a] *Fumin Li,* [a]* *Mengqi Jin,* [a] *Yanjing Rong,* [a] *Xingyuan Tian,* [a] *Rong Liu,* [a]* *Chong Chen*[ab]*

[a] Henan Key Laboratory of Photovoltaic Materials, Henan University, No.1 Jinming Road, Kaifeng, Henan 475004, China.

[b] Institute of Solid State Physics, HFIPS, Chinese Academy of Sciences, Hefei 230031, P. R. China

E-mail: lifm@henu.edu.cn (Dr. Li); rong@vip.henu.edu.cn (Dr. Liu); chongchen@henu.edu.cn (Prof. Chen)

Experimental section

Materials: Formamidine iodide (FAI, 99.9%), methylammonium iodide (MAI, 99. 9%), methyl ammonium bromide (MABr, 99.9%), lead iodide (PbI_2, 99.99%), and 2,2',7,7'-tetrakis (N, N dimethoxyphenylamino)-9,9'-spirobifluorene (spiro-OMeTAD, 98.6%) were both purchased from Advanced Electronic Technology Co., Ltd. Tin oxide (SnO_2, 15 wt% in H_2O colloidal dispersion) was purchased from Alfa Aesar. Potassium fluoride (KF, 99.9%), potassium chloride (KCl, 99%), lead bromide ($PbBr_2$, 99.9%), cesium iodide (CsI, 99.999%,), oleic acid (OA, 99.5%) and oleylamine (OLA, 99.5%) were purchased from Aladdin. Bis(trifluoromethanesulfonyl) imide salt (Li-TFSI, 99.9%), dimethyl sulfoxide (DMSO, 99%), 4-tert-butylpyridine (tBP, 98%), and N,Ndiethylformamide (DMF, 99%) were purchased from Sigma-Aldrich. Gold (Au, 99.999%) were purchased from China New Metal Materials Technology Co.

M-QDs synthesis: Under stirring at room temperature, 24.5mg of MABr and 80.5 mg of $PbBr_2$ were added into 500 μL of DMF until dissolved completely. Then 20μL of oleylamine was added. After thorough mixing, a clear solution was obtained, denoting as *Solution I*. Meanwhile, 180 μL of oleic acid was added into 8 mL toluene solution under vigorous stirring for 30 min at room temperature to obtain *solution II*. During the continuous vigorous stirring of *solution II*, *solution I* was added, and the color of the mixed solution changed to yellow instantly. After being centrifuged at 4000 rpm for 20 min, the M-QDs solution of the green supernatant was obtained. Significantly, there is a trace amount of DMF including in the M-QDs solution, and the concentration of M-QDs in the green solution is quantified as about 9 mM. In detail, firstly, a clean dish was weighed. Secondly, 2 mL of the green supernatant was dropped onto the dish and dried naturally to obtain the M-QDs solids. Finally, the dish containing M-QDs solids was weighed again. The D-value between the two weighed results is the mass of the M-QDs, which

is about 8.8 mg. Therefore, the concentration of M-QDs in the green supernatant was inferred to be about 9 mM. In addition, the required concentration of M-QDs in our experiments was obtained by diluting using toluene.

Device fabrication: The ITO glasses were washed consecutively in detergent, deionized water, acetone, and isopropanol by sequential sonication, dried, and treated with ultraviolet ozone (UVO) for 15 min. The SnO_2-KCl colloidal dispersion liquid, the KF aqueous solution, the perovskite precursor, the M-QDs solution, and the Spiro-OMeTAD solution were prepared according to our recent work.[1] On the clean ITO substrates, the SnO_2-KCl liquid was spin coated at 5500 rpm for 10 s and then the films were heated at 150 °C for 10 min and UVO treated for 60 min to obtain an electron transport layer. The KF solution was spin coated at 3000 rpm for 10 s and annealed at 120 °C for 10 min. The perovskite precursor were then spin coated onto the substrates in a N_2-filled glove box, consisting of a two-step program at 1000 and 4500 r.p.m. for 5 and 20 s, respectively. During the second step, 1 ml of ethyl ether was poured on the spinning substrate 5 s before the end of the program. Immediately, the substrates annealed at 120 °C for 10 min. After cooling down to room temperature, the M-QDs solution with different concentrations (0, 0.15, 0.3, 0.45 and 0.6 mM, respectively) was spin coated onto the samples at 5000 rpm for 30 s without any further heat treatment for passivation. After that, a spiro-OMeTAD solution was spin coated at 4500 rpm for 20 s to obtain a hole transport layer. Finally, the device with a structure of ITO/SnO_2-KCl/KF/ CFM/*x*M-QDs (*x* = 0, 0.15, 0.3, 0.45 and 0.6 mM) /Spiro-OMeTAD/Au were completed by thermal evaporation of an Au counter electrode on an active area of 0.04 cm^2 by a shadow mask.

Characterization: The TEM images were characterized by JEOL JEM-F200 transmission electron microscope (Nippon Electronics Co., Japan). The SEM images were obtained using a JSM7001F

field-emission scanning electron microscope (Japan Electron Optics Laboratory Co., Japan), and grain size was measured by the Nano Measure 1.2 software. AFM and KPFM measurements was performed on a Dimension Icon scanning probe microscopy (Bruker, USA). The XRD patterns was measured by a D8-ADVANCE X-ray diffractometer (Bruker, Germany). UV-vis absorption spectra were conducted by Carry 5000 ultraviolet/visible spectrophotometer (Agilent Technologies, China). The PL and TRPL spectra were carried out via a HORIBA Jobin Yvon Fluorolog-3 Spectrofluorometer system and a FLS 980 PL spectrometer (Edinburgh Instrument, England), respectively. The IR spectra were carried out via a VERTEX 70 fourier transform infrared spectroscopy (Bruker, Germany). *J-V* characteristics were measured using a Keithley 2410 source meter (Cleveland, OH, USA) at AM 1.5G illumination (1000 W/m^2) generated by a Newport 94043A solar simulator (USA) and calibrated using a certified silicon solar cell by NREL, including forward scans (FS, from -0.20 to 1.20 V) and reverse scans (RS, from 1.20 to -0.20 V). In addition, The long-term stability test is carried out by performing an *J-V* test at regular intervals on the samples which are placed in three different conditions for a long period of time. IPCE spectra were measured in air by the Qtest Station 500ADX quantum efficiency test system (United States Dawn Technology Co., Ltd., USA). The water contact angle was measured using LAUDA OSA100 fiber optical contact angle tensiometer (LAUDA Scientific GmbH, China). SCLC, M-S, and EIS measurements were carried out via a CHI660E electrochemical workstation (Chenhua Equipment Company, Shanghai, China). The EIS was simulated using Z-View software. Notably, the SEM, AFM, KPFM, XRD, UV−vis, PL, TRPL, FTIR and the water contact angle characterizations are carried out on the films with structure of ITO/SnO_2-KCl/KF/CFM/*x*M-QDs, the *J-V*, dark *J-V*, M-S, and EIS measurements are based on the device of ITO/SnO_2-KCl/KF/CFM/*x*M-QDs/Spiro-

OMeTAD/Au, the SCLC measurement is based on a hole only device of ITO/PTAA/Al_2O_3/CFM/*x*M-QDs/Spiro-OMeTAD/Au, and the electrical conductivity test is carried out between ITO and Au on the films of ITO/*x*M-QDs/Au.

First-principles calculations: Electronic structure calculations are performed with the density functional theory as implemented in the Vienna ab initio simulation package,[2, 3] employing projected augmented wave potentials to describe the atomic core electrons and a plane wave basis set with a kinetic energy cutoff of 450 eV to expand the Kohn−Sham electronic states. For the exchange and correlation functional, the generalized gradient approximation (GGA) in the Perdew–Burke–Ernzerhof (PBE) format was used.[4]

The CFM/OLA interface was simulated by a periodic slab model. Firstly, a 3 × 1 $CH_3NH_3PbI_3$ (001) surface unit cell with 6 atomic layers was constructed, and a vacuum thickness of 20 Å was added along the z direction. Then the OLA molecule was deposited on the $CH_3NH_3PbI_3$ (001) surface. The Brillouin zone was sampled in (1 × 3 × 1) and (3 × 5 × 1) Monkhorst–Pack grids,[5] respectively, in the structure relaxations and density of states (DOS) calculations. The dispersion correction was also included by the DFT+D2 scheme.[6] To reduce computational cost and mimic the bulk influence, the bottom 4 atomic layers of $CH_3NH_3PbI_3$ were fixed during structural optimization, and other atomic layers and the OLA molecule were relaxed until the atomic forces are smaller than 0.05 eV Å-1.

Supplementary Figures

Fig. S1. Green fluorescence of M-QDs solution under 365nm UV light irradiation.

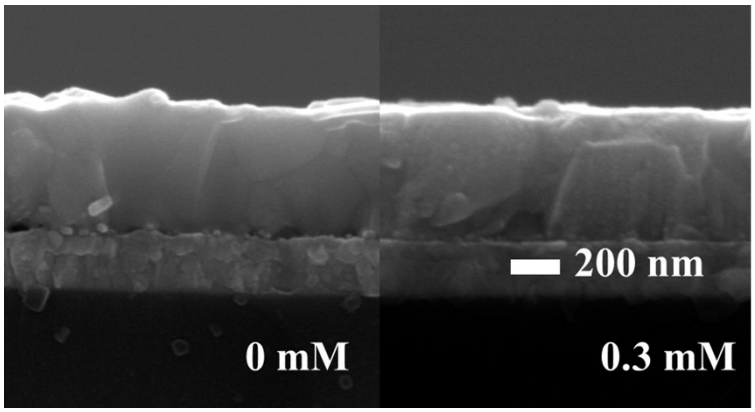

Fig. S2. Cross-section SEM of ITO/SnO_2-KCl/KF/CFM and ITO/SnO_2-KCl/KF/CFM/M-QDs (0.3 nM) films

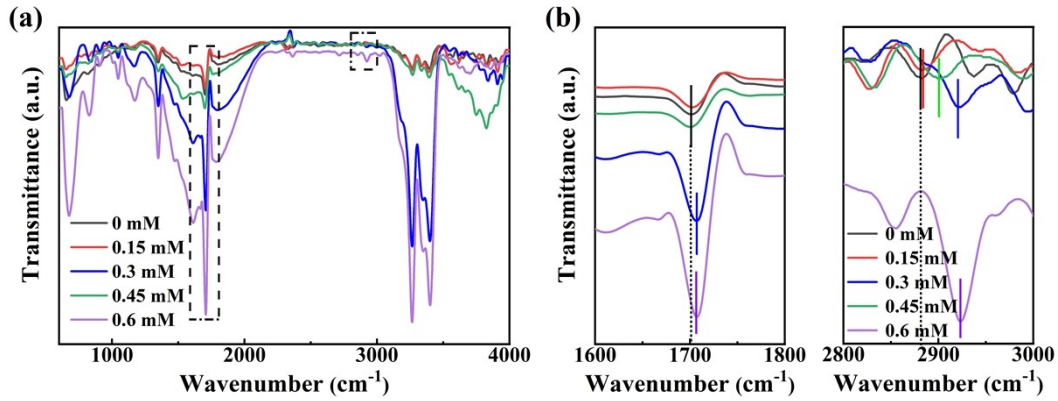

Fig. S3. (a) FTIR spectra of the ITO/SnO_2-KCl/KF/CFM/M-QDs films passivated with different concentrations of M-QDs. (b) Enlarged view of 1600cm^{-1}-1800cm^{-1} and 2800cm^{-1}-3000cm^{-1} from the FTIR spectra in (a).

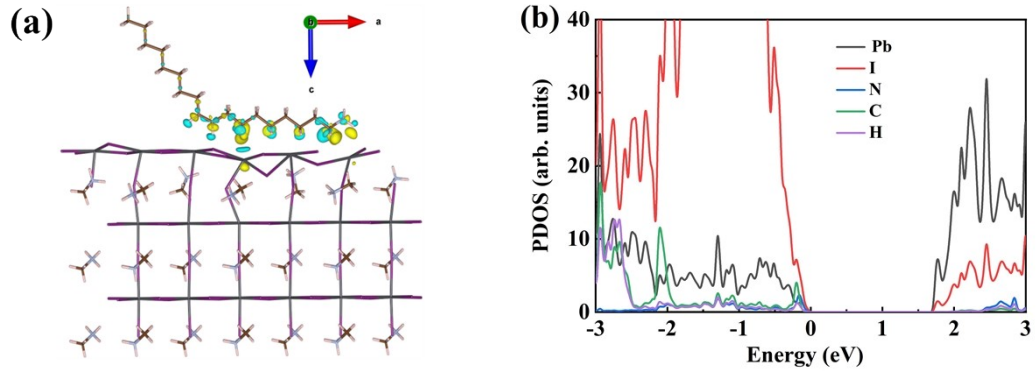

Fig. S4. (a) Interfacial bonding interaction at the CFM/OLA interface observed along the (001) direction. (b) The partial density of states (PDOS) of the CFM/OLA interface.

Note for Fig. S4: There is a strong interaction between NH_2 group on the OLA molecular chains and Pb atoms of the CFM, and the electrons on the OLA molecular chain and the holes on the Pb atoms in perovskite aggregate simultaneously to the CFM/OLA interface, forming an interfacial electric field along the c axis, which will be very helpful for the hole transfer from the perovskite to the spiro-OMeTAD layer[7]. Therefore, OLA not only has good hydrophobic function, but also stabilizes the chemical stability of perovskite materials to a certain extent.

Table S1. Fitted parameters of TRPL spectra of perovskite films passivated with different concentrations of M-QDs. The τ_{avg} is calculated from the equation of $\tau_{avg}=(A_1*\tau_1^2+A_2*\tau_2^2)/ (A_1*\tau_1+A_2*\tau_2)$.[7]

	τ_1 (ns)	A_1 (%)	τ_2 (ns)	A_2 (%)	τ_{avg} (ns)
0 mM	93.1	80.62	1005.24	19.38	751.59
0.15 mM	123.46	79.83	855.73	20.17	589.53
0.3 mM	63.74	77.14	528.04	22.86	393.63
0.45 mM	129.18	79.68	771.49	20.32	516.89
0.6 mM	125.28	77.38	893.9	22.62	644.81

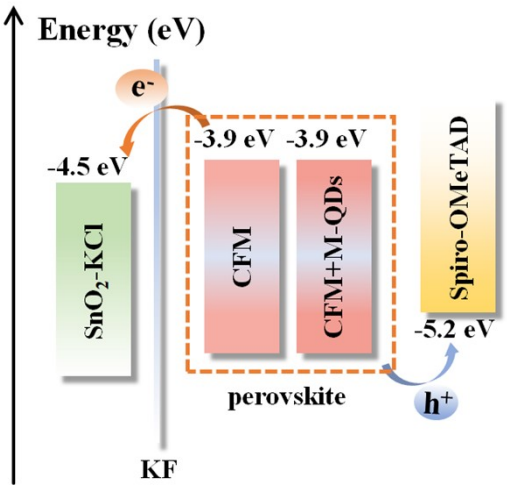

Fig. S5. The energy level alignment of SnO_2-KCl/KF/Perovskite/HTL

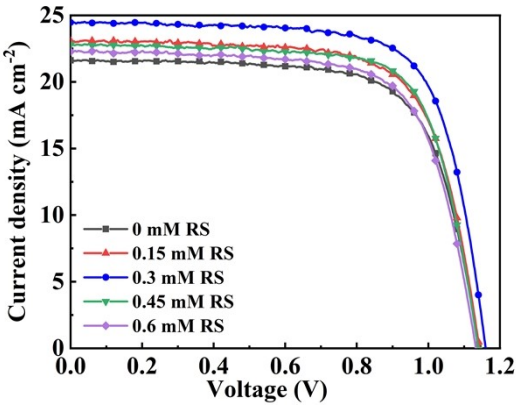

Fig. S6. Reverse scan current density-voltage (*J-V*) curves of ITO/SnO_2-KCl/KF/CFM/*x*M-QDs /Spiro-OMeTAD/Au solar cells.

Table S2. Summary of photovoltaic performance parameters over reverse scan (RS) *J-V* curve of ITO/SnO_2-KCl/KF/CFM/*x*M-QDs/Spiro-OMeTAD/Au solar cells.

	V_{oc} (V)	J_{sc} (mA cm^{-2})	PCE (%)	FF (%)	HI (%)
0 mM	1.14	21.62	17.37	70.49	7.75
0.15 mM	1.14	23.07	18.55	70.54	5.89
0.3 mM	1.16	24.46	20.47	72.15	2.24
0.45 mM	1.14	22.82	18.83	72.37	3.68
0.6 mM	1.13	22.27	17.72	70.41	4.47

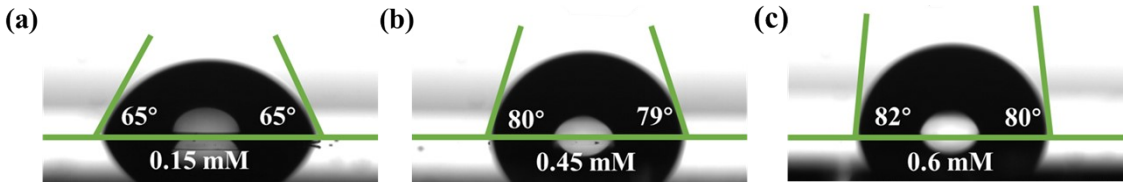

Fig. S7. The water contact angles of the perovskite films passivated with different concentrations of M-QDs (a) 0.15mM, (b) 0.45mM, and (c) 0.6mM.

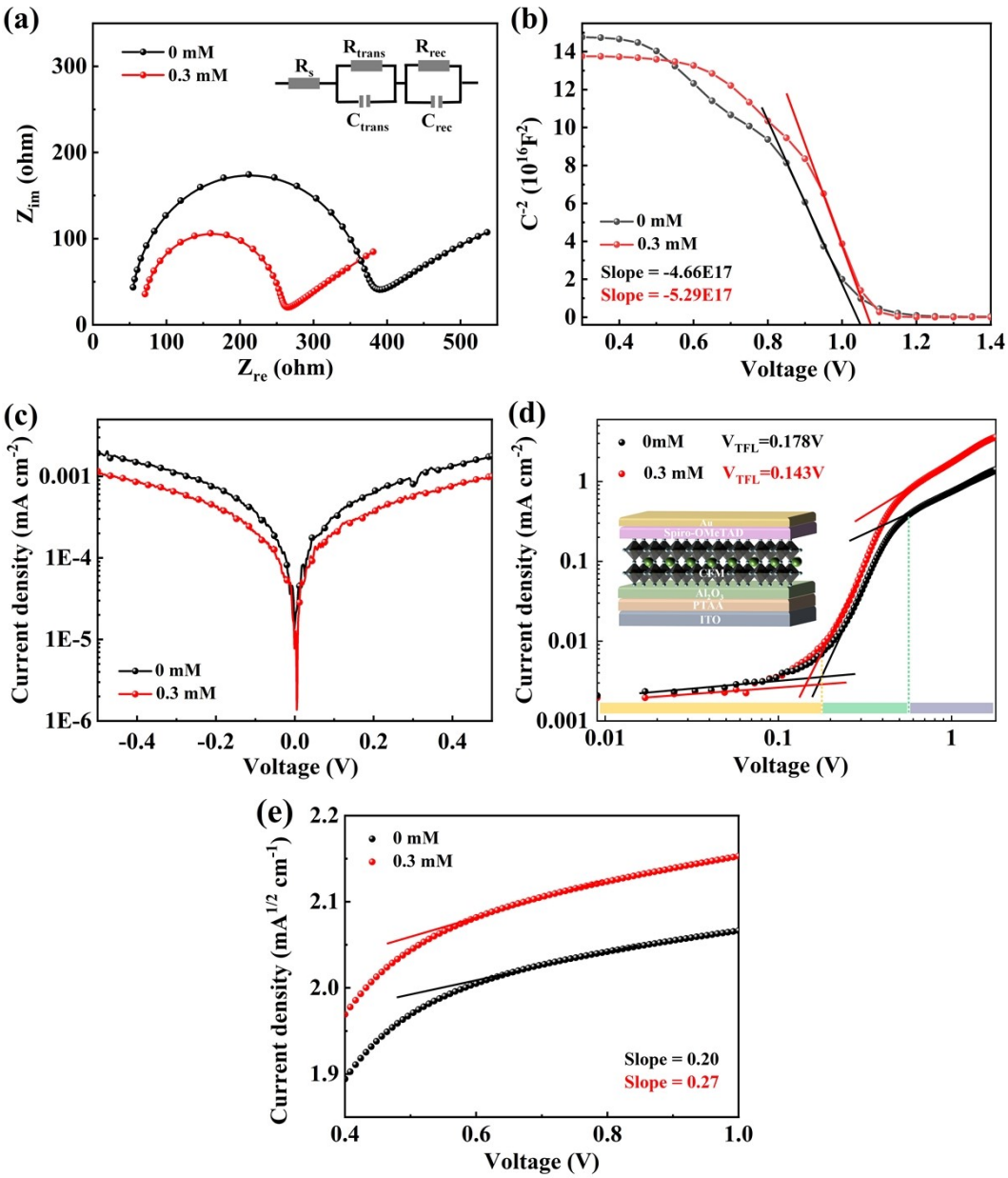

Fig. S8. (a) EIS (The inset shows the equivalent circuit of PSCs), (b) *M-S* diagram, and (c) *J-V* characteristics scanning from -0.5V to 0.5V in the dark of the optimal and control devices. (d) The *J-V*

and (e) $J^{1/2}$–V characteristics of hole-only devices by space charge limited current model with a structure of ITO/ PTAA/Al_2O_3/CFM/M-QDs (0 and 0.3 mM)/Spiro-OMeTAD/Au.

Note for Fig. S8d and S8e: The calculations of defect density states are according to equation[8] $n_{trap} = 2V_{TFL}\varepsilon_r\varepsilon_0/eL^2$, and the hole mobility (μ_h) can be calculated by the Mott-Gurney law[1, 9] of $J = (9/8)\varepsilon_r\varepsilon_0\mu_h V^2L^{-3}$, where ε_0 is the vacuum permittivity of perovskite layer (about 8.8542×10^{-12} F/m), ε_r is relative dielectric constant of perovskite layer (about 47), e is the elementary charge and L is the thickness of the perovskite layer (about 500 nm). For the CFM device, the values of V_{TFL} , n_{trap} and μ_h are calculated as 0.178 V, 3.71×10^{15} cm^{-3} and 1.07×10^{-3} cm^2 V^{-1} S^{-1}, respectively. And for the CFM/M-QDs (0.3 mM) device, the values of V_{TFL} , n_{trap} and μ_h are 0.143 V, 2.98×10^{15} cm^{-3} and 1.95×10^{-3} cm^2 V^{-1} S^{-1}, respectively.

Table S3. EIS fitting results for the optimal and control devices.

	R_s (Ω cm^2)	R_{trans} (Ω cm^2)	R_{rec} (Ω cm^2)	C_{trans} (μF cm^{-2})	C_{rec} (μF cm^{-2})
0 mM	66.07	302.2	827.9	1.06	0.44
0.3 mM	48.80	177.0	1342.0	1.09	0.40

References

1 Y. Feng, R. Liu, F. Li, M. Jin, Q. Du, Y. Rong, H. Hu, M. Wang, Y. Li, Z. Shen, Y. Liu, H. Li and C. Chen, *J. Mater. Chem. C*, 2022, **10**, 12699-12707.

2 G. Kresse and J. Hafner, *Phys. Rev. B*, 1993, **47**, 558-561.

3 G. Kresse, *Phys. Rev. B*, 1996, **54**, 11169-11186.

4 K. B. John P. Perdew, * Matthias Ernzerhof, *Phys. Rev. Lett.*, 1996, **77**, 3865-3868.

5 H. J. Monkhorst and J. D. *Phys. Rev. B: Solid State*, 1976, **13**, 5188-5192.

6 S. Grimme, *J. Comput. Chem*, 2006, **27**, 1787-1799.

7 C. Chen, F. Li, L. Zhu, Z. Shen, Y. Weng, Q. Lou, F. Tan, G. Yue, Q. Huang and M. Wang, *Nano Energy*, 2020, **68**, 104313-104324.

8 Q. Du, Z. Shen, C. Chen, F. Li, M. Jin, H. Li, C. Dong, J. Zheng, M. Ji and M. Wang, *Solar RRL*, 2021, **5**, 2100622-2100631.

9 G.-J. A. H. Wetzelaer, M. Scheepers, A. Miquel Sempere, C. Momblona, J. Avila, H. J. Bolink, *Adv. Mater.*, 2015, **27**, 1837.